A Wavelet-Based FDTD-Multigrid-Method

Marc Walter, Peter Waldow and Ingo Wolff

Gerhard-Mercator-Universität Duisburg, Department of Electromagnetic Theory and Engineering, Bismarckstr. 81, 47048 Duisburg, Germany

***Abstract*—In the past years, several methods combining FDTD-like algorithms and wavelets have been developed in order to reduce simulation times. We present a method that directly transforms Yee's three-dimensional FDTD-algorithm into the wavelet domain at arbitrary scale. We derive an analytic and stable multigrid-like method and present simulation results.**

I. Introduction

Simulation algorithms like the FDTD-method [1] enable researchers and developers to analyse the electromagnetic properties of waveguides, antennas and other objects. Unfortunately, these objects sometimes have to be discretized very fine in time and space in order to get results of reasonable precision. Mostly the small discretization steps are necessary only at edges and similar zones where field components have high gradients. Several multigrid methods have been derived which allow to limit the small discretization steps to the problematic regions. These methods often lack numerical stability.

Another approach is to take advantage of compression properties of wavelet transforms [2] which are very efficient for image compressions. The wavelet analysis allows to observe data (functions, singals, etc.) on different scales (resolutions). Omitting "unimportant" details and preserving the "important" ones in some regions leads to a compression which, in some aspects, is similar to multigrid compression. We show how this can be incorporated into the FDTD algorithm and that this approach leads to an analytic and stable multigrid-like method. Furthermore, we can show that our method can be applied not only to the FDTD algorithm, but to every linear algortihm (TLM [3] and MRTD [4], e.g.).

Our first approach presented in [5] was based on matrix-vector-multiplications: The three-dimensional fields and structure data (dielectric constants, boundaries) were regarded as different sets of vectors. Then, matrices known from the wavelet-based multiresolution analysis could be used to transform the fields and structure data into the wavelet domain. This method is relatively easy to implement. Unfortunately, inhomogeneities require dissections of the structure data into sub-homogeneous parts and the implementation of masking matrices. Although all matrices are sparse inefficiencies can occur due to the increasing number of dissections necessary for an increasing number of inhomogeneities. In [5] we discussed these difficulties and announced the development of another approach which we now want to present.

II. Theory

On a cartesian mesh with Yee-cells at discrete points addressed with the integer triple (i,j,k) the relations between all field components look similar to the following one:

$$\begin{aligned} E_x^{n+1}(i,j,k) &= E_x^n(i,j,k) \\ &+ c_1^{E_x}(i,j,k)\frac{H_z^{n+\frac{1}{2}}(i,j,k) - H_z^{n+\frac{1}{2}}(i,j-1,k)}{\Delta y} \\ &+ c_2^{E_x}(i,j,k)\frac{H_y^{n+\frac{1}{2}}(i,j,k) - H_y^{n+\frac{1}{2}}(i,j,k-1)}{\Delta z}, \end{aligned} \quad (1)$$

with the constants $c_2^{E_x}$ and $c_1^{E_x}$ incorporating time step width and material properties at (i,j,k). Δy and Δz are the space steps in y- and z-direction, n is the number of the time step. All operations in equation (1) are linear and can hence be expressed with linear operators.

In general, we consider functions of the form

$$g_\mu(\mathbf{r}) = \sum_\nu \sum_\eta c_{\mu,\eta}^\nu(\mathbf{r}) f_\nu(\mathbf{r}_{\mu,\eta}^\nu(\mathbf{r})) \,, \quad (2)$$

where μ and ν denote components of the fields g and f, $\mathbf{r}$ points to an element of the discretized space and c denotes a factor. In operational form and for all components μ, ν at all points $\mathbf{r}$ equation (2) can be written as

$$\mathcal{G} = \mathcal{O}\mathcal{F} \,, \quad (3)$$

where $\mathcal{O}$ is a linear operator transforming field $\mathcal{F}$ to field $\mathcal{G}$. Extending Yee's method with further linear algorithms (Berenger's PML or Mur's boundary conditions, e.g., [6]) and applying the notation of equation (3) leads to

$$\mathcal{H}^{n+\frac{1}{2}} = \mathcal{O}^{\mathcal{H}}_{\mathcal{H}}\mathcal{H}^{n-\frac{1}{2}} + \mathcal{O}^{\mathcal{H}}_{\mathcal{E}}\mathcal{E}^{n}, \tag{4}$$

$$\mathcal{E}^{n+1} = \mathcal{O}^{\mathcal{E}}_{\mathcal{E}}\mathcal{E}^{n} + \mathcal{O}^{\mathcal{E}}_{\mathcal{H}}\mathcal{H}^{n+\frac{1}{2}}, \tag{5}$$

where all operators are linear. We can thus restrict our further considerations to equation (3).

The wavelet transform, especially multi resolution analysis (MRA), is linear, too. For one-dimensional signals $\mathbf{v}$, a matrix $\mathbf{P} = \mathbf{P}^{0,J}$ enables to transform the signal vector from scale 0 ("fine"=original scale) into the wavelet domains up to scale J ("coarse" scale) applying a matrix-vector multiplication $\mathbf{v} \cdot \mathbf{P}$. This matrix can simply be extended to an operator $\mathcal{P}^{0,J}$ that performs the one-dimensional wavelet transform for a three-dimensional vector field. An operator $\mathcal{P}$ for a wavelet transform to all directions is then

$$\mathcal{P} = \mathcal{P}^{0,J_x}\mathcal{P}^{0,J_y}\mathcal{P}^{0,J_z}\,, \tag{6}$$

and its inverse operator will be denoted $\mathcal{Q}$. The wavelet transform of equation (3) then results in

$$\hat{\mathcal{G}} = \hat{\mathcal{O}}\hat{\mathcal{F}}\,, \tag{7}$$

with

$$\hat{\mathcal{G}} = \mathcal{P}\mathcal{G}, \quad \hat{\mathcal{F}} = \mathcal{P}\mathcal{F}, \quad \hat{\mathcal{O}} = \mathcal{P}\mathcal{O}\mathcal{Q}. \tag{8}$$

In the same way equations (4) and (5) can be transformed.

In [5] we performed the realisation of equation (7), especially the realisation of the operator $\hat{\mathcal{O}}$, with matrix-vector multiplications as mentioned above. Our new approach uses the direct concatenation of operators with the help of equation (2): Each operator is defined by its factor- and vector-components $c^{\nu}_{\mu,\eta}(\mathbf{r})$ and $\mathbf{r}^{\nu}_{\mu,\eta}(\mathbf{r})$. Concatenating an operator $\mathcal{A}$ (${}_{a}c^{\nu}_{\mu,\eta}(\mathbf{r})$, ${}_{a}r^{\nu}_{\mu,\eta}(\mathbf{r})$) with operator $\mathcal{B}$ (${}_{b}c^{\nu}_{\mu,\eta}(\mathbf{r})$, ${}_{b}r^{\nu}_{\mu,\eta}(\mathbf{r})$) leads to operator $\mathcal{C} = \mathcal{A}\mathcal{B}$ (${}_{c}c^{\nu}_{\mu,\eta}(\mathbf{r})$, ${}_{c}r^{\nu}_{\mu,\eta}(\mathbf{r})$). In general, the principle of concatening the two operators belongs to procedure of writing down an operation $\mathcal{F} = \mathcal{B}\mathcal{H}$ in the form of equation (2) and inserting the resulting equation into equation (2).

It is clear that this procedure can lead to a number of non-vanishing factors ${}_{c}c$ that is higher than the sum of the factors ${}_{a}c$ and ${}_{b}c$. In such case, the direct implementation of equation (7), or the transformed equations of (4) and (5), respectively, increases the numerical effort during the simulation. Now, we have to take advantage of the compression properties of wavelet transforms: If a priori is known or assumed that the signals have rather slow variations in most regions and high variations only in a few regions, then a detail grid can be used to reduce the transformed operators. The following steps are necessary and will explain what we mean with detail grid:

1. Choose for the simulation domain of interest where you want to have more details during the simulation (similar to subgridding in multigrid methods).
2. Define an operator $\mathcal{A}$ that keeps the field in the detail regions and omits the field in the rest.
3. Transform the operator into the wavelet domain: $\hat{\mathcal{A}} = \mathcal{P}\mathcal{A}\mathcal{Q}$.
4. Define an operator $\hat{\mathcal{B}}$ that keeps the (transformed) field wherever $\hat{\mathcal{A}}$ leads to (in general) non-zero values. Let $\hat{\mathcal{B}}$ omit values elsewhere. $\hat{\mathcal{B}}$ will then be a kind of masking operator for the (transformed) details.
5. Define an operator $\hat{\mathcal{C}}$ that keeps the transformed field on the coarsest scale, namely the so-called V-space at scale $\mathbf{J} = (J_x, J_y, J_z)$. Let $\hat{\mathcal{C}}$ omit values elsewhere.
6. Finally, define an operator $\hat{\mathcal{D}}$ that keeps the transformed field wherever $\hat{\mathcal{B}}$ or $\hat{\mathcal{C}}$ keep the field. Let $\hat{\mathcal{D}}$ omit values elsewhere.

This procedure leads to a kind of multigrid filter. $\hat{\mathcal{D}}$ will be called the detail grid operator. We can now use $\hat{\mathcal{D}}$ to approximate equation (7) to

$$\tilde{\mathcal{G}} = \tilde{\mathcal{O}}\tilde{\mathcal{F}}\,, \tag{9}$$

with

$$\tilde{\mathcal{G}} = \hat{\mathcal{D}}\mathcal{P}\mathcal{G}, \quad \tilde{\mathcal{F}} = \hat{\mathcal{D}}\mathcal{P}\mathcal{F}, \quad \tilde{\mathcal{O}} = \hat{\mathcal{D}}\mathcal{P}\mathcal{O}\mathcal{Q}\hat{\mathcal{D}}. \tag{10}$$

We can proof that this approach preserves the stability of the FDTD algorithm, if applied to the equations (4) and (5).

III. Simulation results

To validate our approach we first simulated a rectangular waveguide with a dielectric post as inhomogeneity (Fig. 1) using the standard FDTD-method. At the

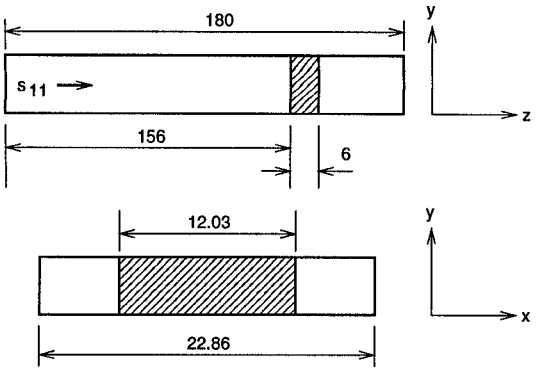

Fig. 1. Simulated structure: air-filled rectangular waveguid with dielectric post ($\varepsilon_r = 8.2$). All dimensions are in mm.

interfaces of the waveguide we placed a Berenger PML as boundary condition. The waveguide was excited with a gaussian TE_{10}-impuls. We thus were able to reduce the three-dimensional problem to two dimensions. The number of timesteps of each simulation was calculated to simulate a physical time of 17.5ns. Fig. 2 shows the simulation results for $|s_{11}|$ for two different space discretizations. Furthermore, measurement results [7] for a very similar structure (dielectric post width 12mm instead of 12.03mm) are shown. We

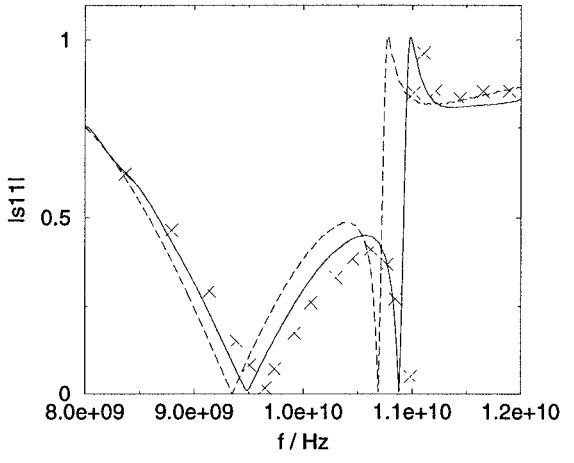

Fig. 2. FDTD simulation results: — for $\Delta x \approx 0.6$mm, $\Delta z = 0.6$mm. - - - for $\Delta x \approx 1.2$mm, $\Delta z = 1.2$mm. Measurements for similar structure: $\times$.

chose to apply our algorithm to the FDTD-operators resulting from the finer discretization. The detail grid was set to cover both PMLs and the dielectric post (plus two elements on each side) over the full cross section. In Fig. 3 we show the results for different scales and different wavelets. As wavelet functions we used the "standard" Daubechies functions D_1 (identical to Haar-basis) and D_2. Table 1 shows the simulation times for all presented simulations. Further experiments with higher scales and/or Daubechies wavelets of higher order showed that calculation times can easily exceed those of pure FDTD simulations. The proper choice of the detail grid has also great influence on the precision of the results. Nevertheless, we were able to show that our approach leads to reasonable results and is able to save simulation time.

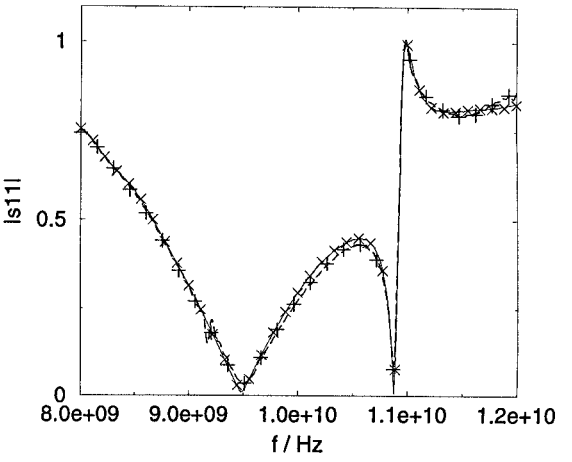

Fig. 3. — : identical to Fig. 2. Simulation results after transformation: + : $(J_x, J_z) = (0,1)$, D_1-basis; $\times$: $(J_x, J_z) = (0,2)$, D_2-basis; - - - : $(J_x, J_z) = (1,1)$, D_1-basis.

J_x	J_z	Δ/mm	Wavelet	Time/s
0	0	1.2	–	5.5
0	0	0.6	–	35.3
0	1	0.6	D_1	25.8
0	2	0.6	D_2	32.8
1	1	0.6	D_1	21.7

Table 1. Simulation times for different space discretizations, scales ($J_x = J_z = 0$ is pure FDTD) and Daubechies functions.

IV. CONCLUSIONS

We presented a method that allows to derive multigrid-like variations of linear algorithms and hence allows to extend well-known and established simulation methods to new classes of problems. We demonstrated this in combination with the FDTD method.

For this case, we can also proof the maintenance of numerical stability. Regarding compression rates for one-dimensional signals and those for images accessible with multi resolution analysis clearly show that MRA techniques gain importance with increasing number of dimensions and size. But despite the "unbalanced" geometry of our test structure we could demonstrate the validity of our approach and its potential to reduce simulation times. Therefore, we will soon analyze problems that fit better in the scheme mentioned above. We are convinced that our method can play an important role on large-scale problems.

REFERENCES

[1] K. S. Yee, "Numerical solution of initial boundary value problems involving Maxwell's equations in isotropic media," *IEEE Antennas and Propagation*, vol. 14, no. 5, pp. 302–307, May 1966.

[2] A. K. Louis, P. Maaß, and A. Rieder, *Wavelets*, Teubner, Stuttgart, 1994.

[3] P. B. Johns, "A symmetrical condensed node for the TLM method," *IEEE Transactions on Microwave Theory and Techniques*, vol. 35, no. 4, pp. 370–377, Apr. 1987.

[4] M. Krumpholz and L. P. B. Katehi, "MRTD: New time-domain schemes based on multiresolution analysis," *IEEE Transactions on Microwave Theory and Techniques*, vol. 44, no. 4, pp. 555–571, Apr. 1996.

[5] M. Walter and I. Wolff, "An algorithm for realizing Yee's FDTD-method in the wavelet domain," in *Microwave Symposium Digest*. IEEE MTT-S International, Anaheim, California, June 1999, Session WEF1-15.

[6] A. Taflove, *Computational Electromagnetics: The Finite-Difference Time-Domain Method*, Artech House, Boston, 1995.

[7] J.-W. Tao and H. Baudrand, "Multimodal variational analysis of uniaxial waveguide discontinuities," *IEEE Transactions on Microwave Theory and Techniques*, vol. 39, no. 3, pp. 506–516, 1991.